Active sites of stoichiometric cerium oxide cations ($Ce_mO_{2m}^+$) probed by reactions with carbon monoxide and small hydrocarbon molecules

Xiao-Nan Wu,[†,‡] *Yan-Xia Zhao,*[†,‡] *Wei Xue,*[†,‡] *Zhe-Chen Wang,*[†,‡] *Sheng-Gui He,*[†,*] *and Xun-Lei Ding*[†,*]

[†]Beijing National Laboratory for Molecular Sciences, State Key Laboratory for Structural Chemistry of Unstable and Stable Species, Institute of Chemistry, Chinese Academy of Sciences, Beijing 100190, P. R. China. [‡]Graduate School of Chinese Academy of Sciences, Beijing 100039, P. R. China.

Contents

Table S1: DFT calculated and experimental ionization and (or) bond dissociation energies of cerium oxides and some related main group species.

A more detailed consideration of the computational accuracy.

Fig. S1: DFT optimized isomeric structures and energies of $Ce_3O_6^+$ cluster.

Fig. S2: DFT optimized isomeric structures and energies of $Ce_4O_8^+$ cluster.

Fig. S3: One structure of $Ce_5O_{10}^+$ cluster optimized by DFT.

Fig. S4: TOF mass spectra for reactions of $Zr_2O_{3-5}^+$ with CH_4 and C_2H_6.

Fig. S5: DFT calculated HOMOs of CeO_2 and ZrO_2, and SOMOs of $CeAl_3O_7$, $CeSi_3O_{10}H_3$, CeV_3O_{10}, and CeP_3O_{10} neutral clusters.

Table S1: DFT calculated and experimental ionization (IE in eV) and (or) bond dissociation (D_0 / $\Delta H_{298\mathrm{K}}$ in eV) energies of cerium oxides and some related main group species.

	DFT		Experiment[a]	
	B3LYP	BPW91	IE or D_0	Reference
$^3\mathrm{Ce} \rightarrow {}^4\mathrm{Ce}^+ + e^-$	5.47	5.38	5.5387 ± 0.0004	1
$^3\mathrm{CeO} \rightarrow {}^2\mathrm{CeO}^+ + e^-$	5.45	5.30	4.9 ± 0.1	2
$^3\mathrm{CeO} \rightarrow {}^3\mathrm{Ce} + {}^3\mathrm{O}$	8.02	8.42	8.2±0.1	3
$^2\mathrm{CeO}^+ \rightarrow {}^4\mathrm{Ce}^+ + {}^3\mathrm{O}$	8.03	8.50	8.8±0.2	4
$^1\mathrm{CeO}_2 \rightarrow {}^3\mathrm{CeO} + {}^3\mathrm{O}$	6.20	7.14	6.7±0.2	5
$^2\mathrm{CeO}_2^+ \rightarrow {}^2\mathrm{CeO}^+ + {}^3\mathrm{O}$	3.15	4.14	> 3.18	8
$^2\mathrm{Ce}_2\mathrm{O}_3^+ \rightarrow {}^2\mathrm{Ce}_2\mathrm{O}_2^+ + {}^3\mathrm{O}$	5.56	6.64		
$^2\mathrm{Ce}_2\mathrm{O}_3^+ \rightarrow {}^4\mathrm{Ce}_2\mathrm{O}_2^+ + {}^3\mathrm{O}$	5.52	6.49		
$^2\mathrm{Ce}_2\mathrm{O}_4^+ \rightarrow {}^2\mathrm{Ce}_2\mathrm{O}_3^+ + {}^3\mathrm{O}$	2.52	3.50		
$^2\mathrm{Ce}_2\mathrm{O}_4^+ \rightarrow {}^2\mathrm{Ce}_2\mathrm{O}_2^+ + 2\,{}^3\mathrm{O}$	8.09	10.13		
$^1\mathrm{CH}_4 \rightarrow {}^2\mathrm{CH}_3 + {}^2\mathrm{H}$	4.48	4.40	4.54	7
$^1\mathrm{C}_2\mathrm{H}_6 \rightarrow {}^2\mathrm{C}_2\mathrm{H}_5 + {}^2\mathrm{H}$	4.25	4.15	4.36	7
$^2\mathrm{OH} \rightarrow {}^3\mathrm{O} + {}^2\mathrm{H}$	4.40	4.42	4.44	7
$^1\mathrm{CH}_3\mathrm{CHO} \rightarrow {}^1\mathrm{C}_2\mathrm{H}_4 + {}^3\mathrm{O}$	4.70	5.00	4.90	7
$^1\mathrm{CO}_2 \rightarrow {}^1\mathrm{CO} + {}^3\mathrm{O}$	5.50	5.97	5.52	7
$^3\mathrm{O}_2 \rightarrow 2\,{}^3\mathrm{O}$	5.15	5.81	5.17	7

[a] The experimental data with relatively small uncertainties are listed for cerium species (see ref 6 for alternative values). The enthalpies of formation for the main group species are well determined and most of them can be found in NIST Chemistry WebBook.[7]

1 E. F. Worden, R.W. Solarz, J. A. Paisner, J. G. Conway, *J. Opt. Soc. Am.*, 1978, **68**, 52-61.

2 R. J. Ackermann, E. G. Rauh, R. J. Thorn, *J. Chem. Phys.*, 1976, **65**, 1027-1031.

3 Dulick, M.; Murad, E.; Barrow, R. F. *J. Chem. Phys.,* **1986**, *85*, 385-390.

4 M. S. Chandrasekharaiah, K. A. Gingerich, *In Handbook on the Chemistry and Physics of Rare Earths*, Elsevier, Amsterdam, 1989, Vol. 12, Chapter 86.

5 J. Kordis, K. A. Gingerich, *J. Chem. Phys.*, 1977, **66**, 483-491.

6 T. K. Todorova, I. Infante, L. Gagliardi, J. M. Dyke, *Int. J. Quantum. Chem.,* 2009, **109**, 2068-2079.

7 http://webbook.nist.gov/chemistry.

8 C. Heinemann, H. H. Cornehl, D. Schroder, M. Dolg and H. Schwarz, Inorg. Chem., 1996, 35, 2463-2475.

A more detailed consideration of the computational accuracy

Table S1 lists the DFT calculated and experimental ionization (IE) and (or) bond dissociation (D_0) energies of Ce atom, cerium oxides, and some related main group species. The D_0 values of all of the main group species can be well reproduced by the hybrid B3LYP functional with TZVP basis set, while the pure GGA functional BPW91 overestimates the D_0 values of CO_2 and O_2 by 0.45 and 0.64 eV, respectively. The B3LYP underestimates the D_0 values of the cerium oxide species listed in Table S1. The underestimation is small for D_0 of CeO (and possibly CeO_2^+) and is by 0.8 eV (or 10%) for that of CeO^+. The BPW91 underestimates the D_0 of CeO^+ by 0.30 eV. Since the computations by the post Hartree-Fock methods [such as MP2, CCSD(T), and CASSCF that are likely more accurate than DFT] are too expensive for studying the mechanisms of reactions of $Ce_2O_4^+$ toward various molecules (see below), the calculations by DFT provide an available basis at present to interpret the experimental observations qualitatively. Table S1 indicates that either B3LYP or BPW91 may be used for studying the reaction mechanisms of cerium oxide clusters with related small molecules. In this study, B3LYP is chosen simply because it gives a good reproduction for the well determined bond energies of all the main group species. One may keep in mind that the B3LYP functional tends to underestimate the Ce-O bond energies (by relative values of about 10% and absolute values as large as 0.8 eV) in the analysis of the data.

Another concern about the accuracy of DFT/B3LYP is that standard DFT may have serious shortcomings for the electronic structures of cerium oxides. The standard DFT can model the ground state of bulk CeO_2 reasonably well while it predicts erroneous metallic ground state for reduced Ce_2O_3 that is a strongly correlated system in terms of the electronic structure.[1,2] The cerium oxide clusters Ce_mO_{2m-1} and Ce_mO_{2m} have been recently studied by the DFT+U approach[3] that was developed to overcome the shortcomings of conventional DFT. It has been concluded that the electronic structures of the stoichiometric clusters Ce_mO_{2m} are not very sensitive to the choice of the

U value (standard DFT corresponds $U = 0$) while for the oxygen-deficient clusters Ce_mO_{2m-1}, the electronic properties are very sensitive to the U value.[4] The $Ce_mO_{2m}^+$ clusters in this study are actually oxygen-slightly-rich (averagely by a half O atom) and they are also not strongly correlated systems (like Ce_mO_{2m}). It is thus expected that the adopted B3LYP can reasonably model the electronic structures of $Ce_mO_{2m}^+$ clusters.

References

1 C. W. M. Castleton, J. Kullgren and K. Hermansson, *J. Chem. Phys.*, 2007, **127**, 244704.

2 J. L. F. Da Silva, M. V. Ganduglia-Pirovano, J. Sauer, V. Bayer and G. Kresse, *Phys. Rev. B*, 2007, **75**, 045121.

3 V. I. Anisimov, J. Zaanen and O. K. Andersen, *Phys. Rev. B*, 1991, **44**, 943-954.

4 S. F. Li, H. Q. Lu, P. L. Li, Z. X. Yang and Z. X. Guo, *J. Chem. Phys.*, 2008, **128**, 164718.

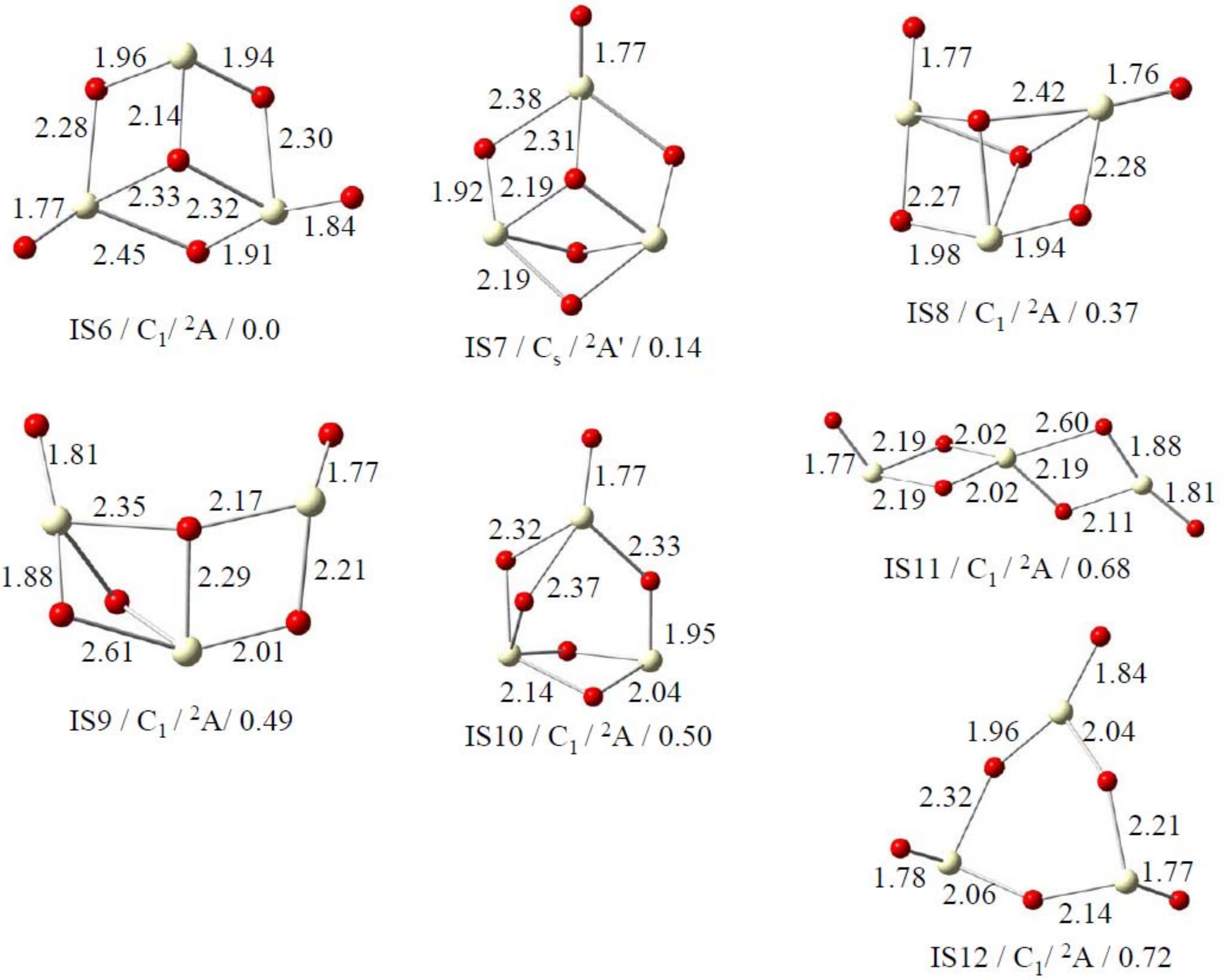

IS6 / C_1 / ^2A / 0.0

IS7 / C_s / $^2A'$ / 0.14

IS8 / C_1 / ^2A / 0.37

IS9 / C_1 / ^2A / 0.49

IS10 / C_1 / ^2A / 0.50

IS11 / C_1 / ^2A / 0.68

IS12 / C_1 / ^2A / 0.72

Fig. S1: DFT optimized isomeric structures (IS6–IS12) and relative energies (in eV) of $Ce_3O_6^+$ cluster. The bond lengths are given in 0.1 nm.

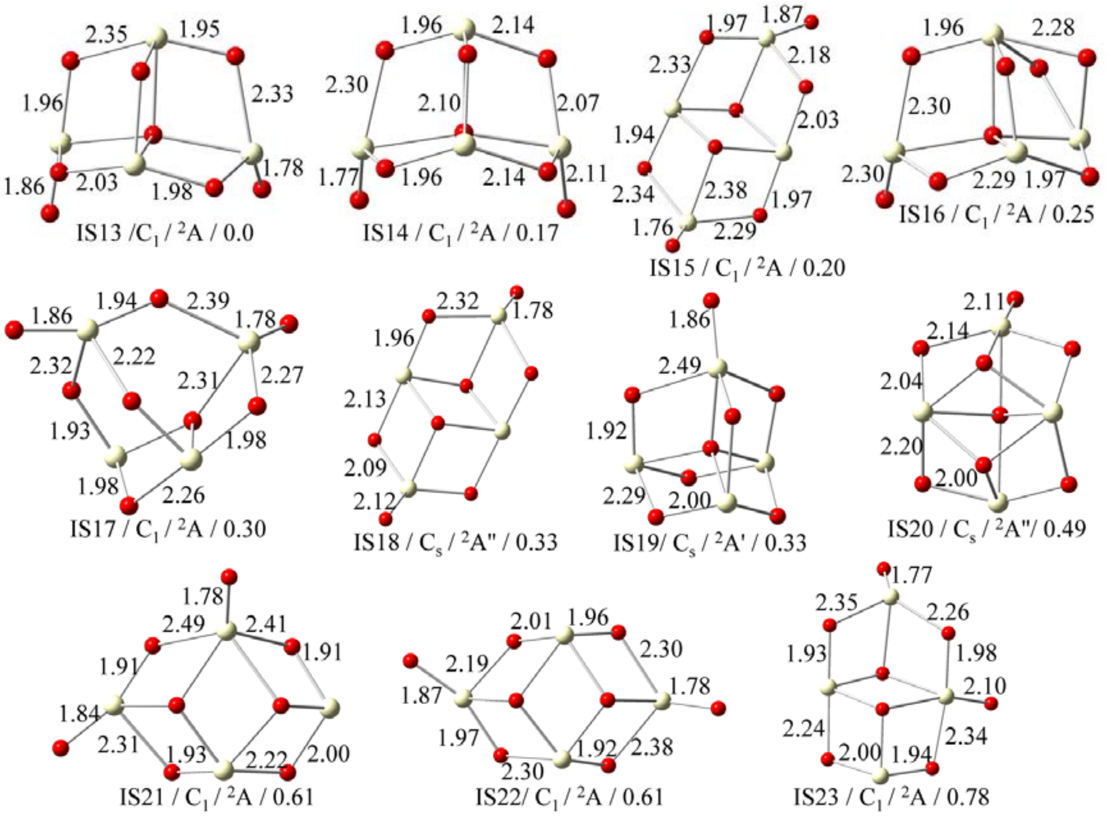

IS13 / C_1 / ^2A / 0.0
IS14 / C_1 / ^2A / 0.17
IS15 / C_1 / ^2A / 0.20
IS16 / C_1 / ^2A / 0.25
IS17 / C_1 / ^2A / 0.30
IS18 / C_s / $^2A''$ / 0.33
IS19 / C_s / $^2A'$ / 0.33
IS20 / C_s / $^2A''$ / 0.49
IS21 / C_1 / ^2A / 0.61
IS22 / C_1 / ^2A / 0.61
IS23 / C_1 / ^2A / 0.78

Fig. S2: DFT optimized isomeric structures (IS13–IS23) and relative energies (in eV) of $Ce_4O_8^+$ cluster. The bond lengths are given in 0.1 nm.

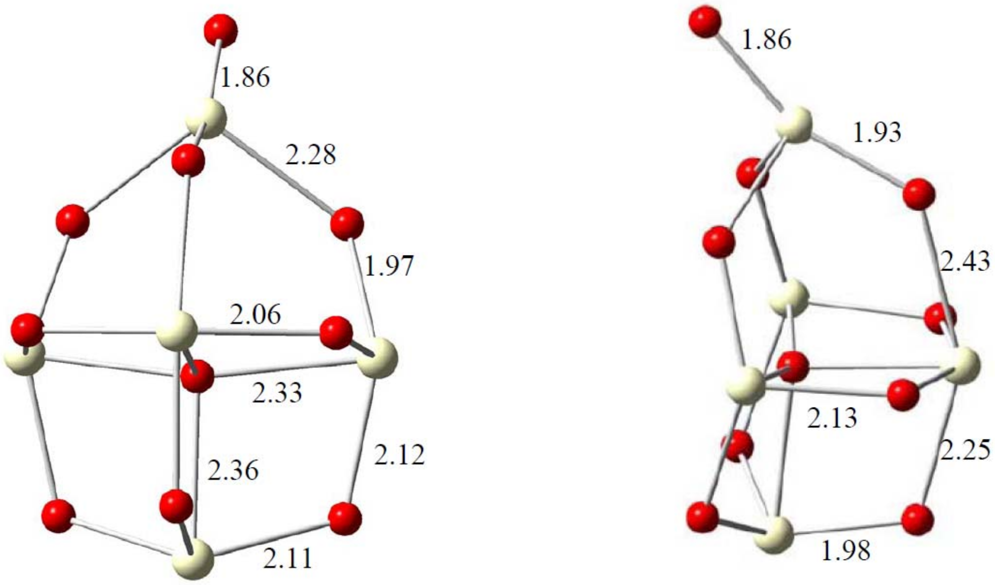

(a) Front view (b) Side view

$Ce_2O_5^+ / C_s / {}^2A'$

Fig. S3: One structure of $Ce_5O_{10}^+$ cluster optimized by DFT. The bond lengths are given in 0.1 nm.

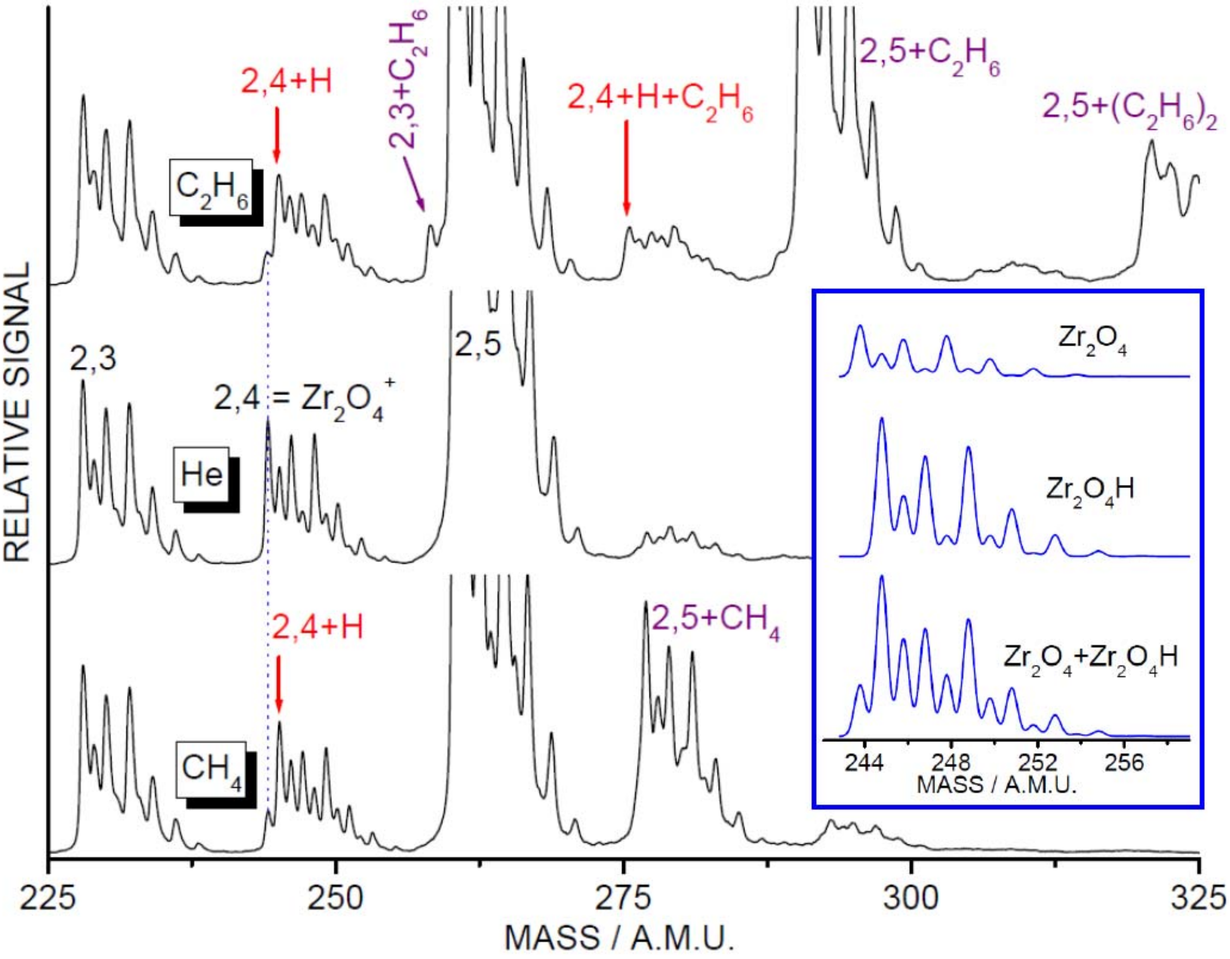

Fig. S4: TOF mass spectra for reactions of $Zr_2O_{3-5}^+$ with He (middle panel), CH_4 (bottom), and C_2H_6 (top). Numbers *m*,*n* denote $Zr_mO_n^+$ and *m*,*n*+X denote $Zr_mO_nX^+$. The isotopic compositions of Zr are as follows: ^{90}Zr (51.45%), ^{91}Zr (11.22%), ^{92}Zr (17.15%), ^{94}Zr (17.38%), and ^{95}Zr (2.80%). On the middle panel of the figure, the first (with the smallest mass) and the second peaks in the $Zr_2O_4^+$ region are assigned as $^{90}Zr_2O_4^+$ (244 amu) and $^{90}Zr^{91}ZrO_4^+$ (245 amu) isotopomers, respectively. After reactions with CH_4 (bottom) and C_2H_6 (top), the intensity of the 244 amu peak ($^{90}Zr_2O_4^+$) decreases while that of the 245 amu ($^{90}Zr^{91}ZrO_4^+$ or $^{90}Zr_2O_4H^+$) increases. This indicates production of $^{90}Zr_2O_4H^+$ from $Zr_2O_4^+$ + CH_4/C_2H_6, which is further supported by the simulation of the isotopic patterns/distributions of Zr_2O_4, Zr_2O_4H, and Zr_2O_4+Zr_2O_4H on bottom-right of the figure.

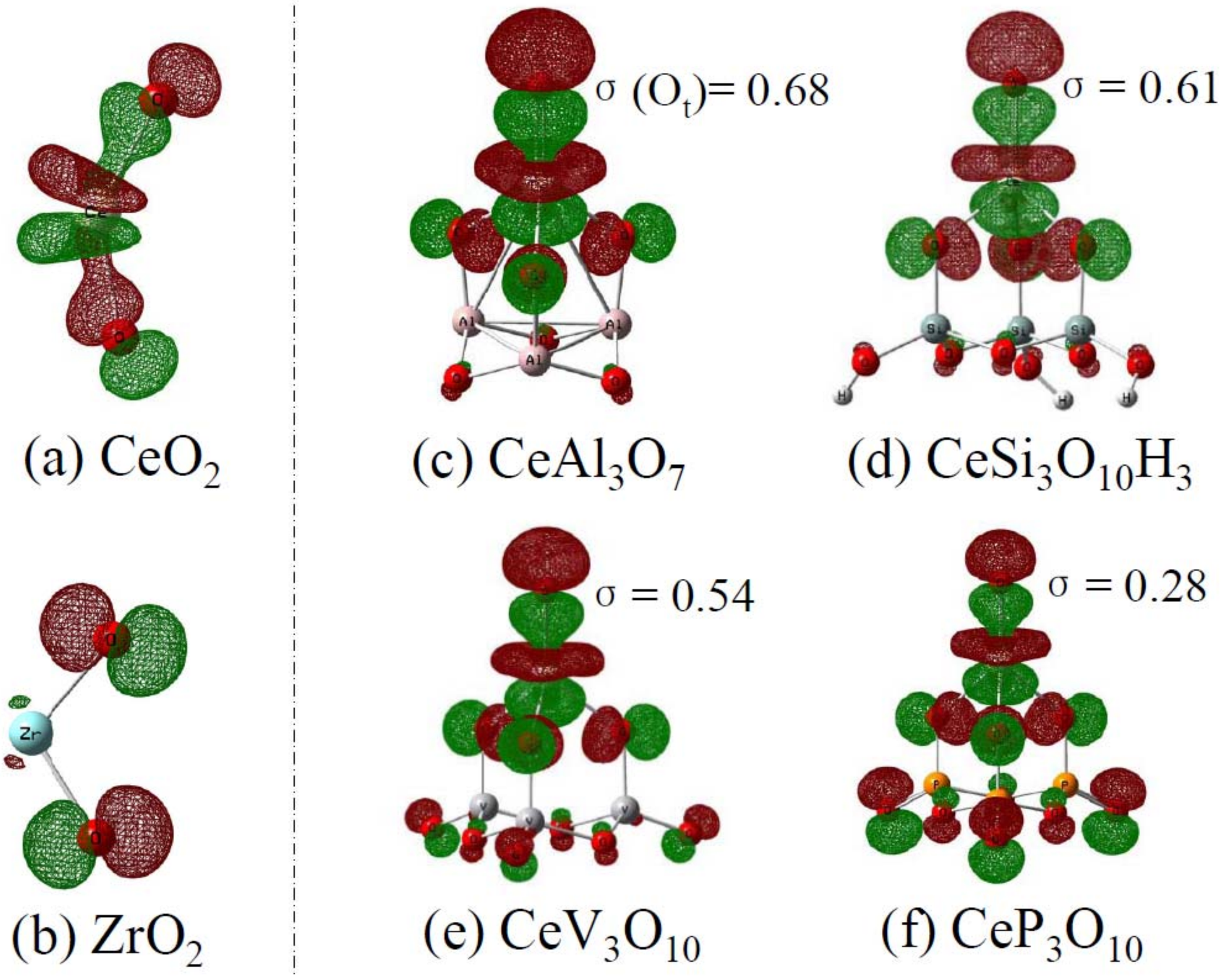

(a) CeO_2 (c) $CeAl_3O_7$ (d) $CeSi_3O_{10}H_3$

(b) ZrO_2 (e) CeV_3O_{10} (f) CeP_3O_{10}

Fig. S5: DFT calculated HOMOs of (a) CeO_2 and (b) ZrO_2, and SOMOs of (c) $CeAl_3O_7$, (d) $CeSi_3O_{10}H_3$, (e) CeV_3O_{10}, and (f) CeP_3O_{10} neutral clusters. Only one typical structure is optimized for each of the clusters in (c–f). The σ values are the spin densities in |e| (or μ_B) over the O_t atom in the Ce-O_t terminal bonds.